BRNO UNIVERSITY OF TECHNOLOGY
FACULTY OF ELECTRICAL ENGINEERING AND COMMUNICATION

DEPARTMENT OF MICROELECTRONICS

TEST METHODS FOR THE EVALUATION OF RADIATION EFFECTS IN HIGH PRECISION ANALOGUE AND MIXED-SIGNAL DEVICES FOR SPACE APPLICATIONS

Summary of doctoral thesis

Author: Ing. Jiří Hofman

Supervisor: doc. Ing. Jiří Háze, PhD

Brno, Harwell, 2019

ABSTRACT

The traditional radiation testing of space electronics has been used for more than fifty years to support the radiation hardness assurance. Its typical goal is to ensure reliable operation of the spacecraft in the harsh environment of space. This PhD research looks into the radiation testing from a different perspective; the goal is to develop radiation testing methods that are focused not only on the reliability of the components but also on a continuous radiation-induced degradation of their performance. Such data are crucial for the understanding of the impact of radiation on the measurement uncertainty of data acquisition systems onboard research space missions.

The thesis is divided into three parts: the first theoretical part contains a discussion of the challenges with designing data acquisition systems for space missions and an overview of the process of estimating measurement uncertainty. It also summarises the theoretical background of the space radiation environment, effects of radiation and temperature on electronic components. The first part concludes with an overview of the traditional radiation hardness assurance and testing.

The second part gives an overview of the new era of a commercial approach to the space technology (NewSpace) and its impact on the radiation hardness assurance and testing processes. A set of advanced in-situ radiation test methods is proposed to address the requirements of the NewSpace and also to provide data with total dose resolution adequate for the development of the models that will be used for live estimation of the measurement uncertainties of data acquisition systems during their missions.

The development of the radiation testing methods and tools is described in the third part of the thesis together with results of various terrestrial total ionising dose tests. A range of commercial electronic components has been tested during the radiation experiments. The experimental campaign started with different types of PMOS devices and continued with precision voltage references and high-resolution A/D converters. The PMOS devices and voltage references were also tested for radiation-induced changes of their temperature coefficients using a novel in-situ measurement method. The third part of the thesis concludes with a description of an in-orbit experiment, which has been designed with a goal to become one of the world's first attempts to measure the impact of the space radiation on a state-of-the-art data acquisition system during spaceflight. The in-orbit experiment has been successfully ground tested for its capability of monitoring total ionising dose, temperature and measuring degradation of various data acquisition components. The in-orbit experiments are expected to be launched on-board two CubeSat missions in the 2020's.

The thesis ends in a conclusion chapter. This chapter summarises both the theoretical and experimental parts of the work. It also provides suggestions for future work and an overview of papers and other presentations published during this PhD programme.

KEYWORDS

Analogue to digital converter, automated test equipment, bias, calibration, CubeSat, data acquisition system, delta-sigma modulation, detector, dosimeter, dosimetry, in-orbit testing, in-situ testing, ionising chamber, measurement, measurement uncertainty, metrology, modelling, multimeter, nanosat, NewSpace, RADFET, radiation, sensor, single event effects, source-measurement unit, space environment, temperature, temperature coefficient, temperature drift, test instrumentation, test software, testing, thermometer, total ionising dose, vacuum, voltage reference.

LOCATION OF THE THESIS

Brno University of Technology, Faculty of Electrical Engineering and Communication. Department of Microelectronics, Technická 3058/10, 616 00 Brno, Czech Republic.

CONTENTS

1 INTRODUCTION

This presented PhD research was focused on the development of test methods enabling the radiation testing for NewSpace low-cost projects including advanced ground and in-orbit experiments. The goal was not only to perform affordable radiation testing but also to possibly change the approach of NewSpace radiation hardness assurance from the classical reliability analysis to continuous, real-time, mission degradation assessments. The proposed test methods were used for components of high-precision space data acquisition systems. The modern components allow the engineers to design commercial data acquisition systems with performance that was previously only achievable by high-tech scientific experiments. Therefore, the ambition of this PhD was to help to bring the powerful commercial data acquisition technologies into space.

1.1 Objectives and motivation

1.1.1 The need for high-resolution COTS data acquisition in space

Space technology has been one of the key contributors to the rapid development of modern astronomy [1]. Despite the great achievements, space-based astronomy missions suffer both a financial and a schedule crisis [2]. The solution to this problem seems to lie in the massive application of commercial technologies (COTS) including commercial parts and rapid design/manufacturing processes. The COTS solutions also offer the remarkable technological level of the commercial components. Although there have been projects aiming to develop space qualified, radiation hardened parts with performance comparable to the COTS, the capabilities of COTS parts are more advanced the employment of rapid commercial development processes.

In conclusion, there is a strong demand for COTS DAQ technologies to be used in the future NewSpace-style scientific missions. Hence, the primary vision of this work is to address the issues related to the applications of the DAQ COTS electronic components and their radiation hardening assurance.

1.1.2 Radiation testing in the era of NewSpace and COTS

The traditional radiation hardening assurance (RHA) is a complex process based on the expected space environment and results from various radiation tests [3]. These datasets are typically obtained from manual component-level testing [4]. Hence, the traditional RHA process is practically impossible to be applied to the NewSpace-style nanosatellites due to budget and time limits. Therefore, the first PhD objective is to design an advanced total ionising dose (TID) radiation testing methods affordable for NewSpace projects. The methods shall be demonstrated on COTS components for DAQ systems.

1.1.3 Real-time mission radiation-induced degradation

The primary goal of traditional RHA is to ensure the reliability of the spacecraft

electronics during the planned lifetime of the mission. However, reliability is only one of the attributes characterising the success of the mission. For scientific missions, the quality of the scientific data is equally important. Hence, there is also a need for modelling of the real-time mission degradation of the performance of space DAQ systems, based on measurements of the radiation environment. Proposal for such a model is the second objective of this PhD work.

1.1.4 Research of synergy between radiation and temperature

Temperature effects have to be carefully considered for the successful design of high-precision DAQ systems [5], [6]. The common term, defining the temperature sensitivity in linear/mixed-signal electronics, is the temperature coefficient *TC* [7].

The traditional RHA literature only discusses the impact of temperature during the irradiation on the magnitude of the radiation-induced changes in the components [3], [8]. Hence, the third PhD objective is to develop and demonstrate a method allowing measurement of radiation-induced changes in *TC* parameters of COTS components for DAQ systems. The resulting data should also be applicable for real-time mission modelling.

1.1.5 In-orbit experiment

A long-term goal of this work is to obtain real in-orbit data to validate the proposed radiation testing methods and models. A broad spectrum of in-orbit experiments has been performed, including various CubeSat projects. A typical goal of these projects was to measure single event effects (SEEs) in various digital components [9]. So far there were missions, observing in-orbit TID effects, however not in DAQ technologies [10]. Therefore the final objective of this PhD work is the development of an in-orbit experiment that can be flown on a nanosatellite (CubeSat).

1.2 Novelty

There are three areas of novelty in this work. Firstly, advanced TID tests methods were developed with the following unique features:

- Fully automated advanced in-situ measurements
- High-resolution test system allowing evaluation of high-precision DAQ components
- High-resolution dose data
- Combined TID and *TC* in-situ testing with unprecedented stability and dynamic response using thermoelectrical technology

Secondly, real-time “live” mission models were developed to estimate the measurement uncertainty of the space DAQ systems during a random moment of the mission.

Thirdly, an in-orbit CubeSat experiment was designed. This project has a potential of introducing a high-tech commercial DAQ technology into the NewSpace scientific missions.

2 SPACE DATA ACQUISITION SYSTEMS

2.1 Influence of space environment on the DAQ system

A typical design of a modern high precision DAQ system is shown in Fig. 2.1. The input signal is firstly processed throughout an analogue signal conditioning stage that commonly consists of a filter, a PGA (Programmable Gain Amplifier) and a MUX (multiplexer). The second stage of the DAQ signal chain is a high-resolution ADC (A/D converter) that uses a reference circuit as a measurement standard. The resulting digital data is communicated to the CPU (Central Processing Unit) which also digitally controls all the programmable parts of the DAQ chain.

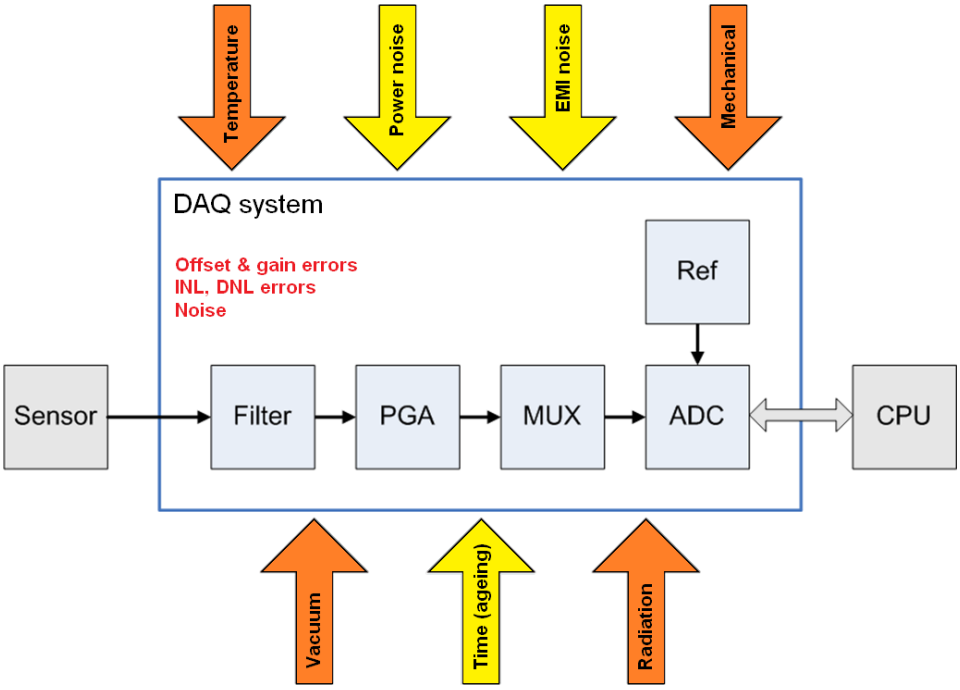

Fig. 2.1: Block diagram of a typical data acquisition system. The DAQ signal chain is shown with its inherent sources of measurement error. When in space, the DAQ system is exposed to harsh environmental conditions as illustrated by coloured arrows.

Every part of the DAQ signal chain is responsible for the overall measurement uncertainty of the entire DAQ system. Therefore, the parasitic properties of these parts are the sources of measurement errors that increase the measurement uncertainty. The typical errors for high precision DC measurements are:

1. offset and gain errors
2. integral (*INL*) and differential (*DNL*) non-linearity errors
3. noise error (measurement repeatability error)

These errors can be identified and ideally suppressed either by calibration or by data processing or by a combination of both. However, these errors are not constant; they drift with the time (ageing) and exhibit a complex dependency on environmental

conditions [5]. Therefore there is a broad spectrum of the environmental conditions that may have a strong influence on the measurement uncertainty of a DAQ system as illustrated by the coloured arrows in Fig. 2.1.

The yellow arrows in Fig. 2.1 represent environmental conditions typical for terrestrial applications, and the orange arrows show the additional influence of the harsh space environment, which not only increases the magnitude of some conditions (temperature, mechanical stress) but also brings new conditions including vacuum and space radiation effects. For practical terrestrial DAQ instruments, the dependency of the measurement error sources on the environmental conditions is typically a key factor for the estimation of measurement uncertainty budgets [6], [11]. Hence, this problem is even more important for space DAQ system as the space environment is even harsher.

2.2 Calibration in space

Traditional calibration of terrestrial DAQ systems is a robust, standardised process consisting of two subsequent stages [12]:

1. initial calibration at the vendor
2. regular calibrations during the lifetime of the DAQ system

Typically, the DAQ system is adjusted during the vendor calibration stage, and the following regular calibrations only check that its measurement errors are within a specification. Should there be a need for an adjustment, it is commonly performed by a change of calibration data stored in the DAQ system. Such a standard calibration process, based on the usage of external traceable calibration instruments, is recognised as a system calibration. This term is often used in the ADC literature [13].

As far as the space DAQ systems on unmanned spacecraft are concerned, the traditional system calibration is limited only to the pre-launch phase of the mission. During the post-launch period, the DAQ system would have to be equipped with additional space-environment-hardened calibration standard should the self-calibration be used to provide similar coverage as of the traditional pre-launch system calibration. In fact, this would make the DAQ hardware significantly more complex. Even the accuracy of the basic offset error self-calibration is not guaranteed in space as the analogue switches, used for shortening the inputs, can suffer radiation-induced enhancement of their parasitic properties including ON-resistance and the leakage currents [14]. The resistor-ladder linearity self-calibration can suffer a similar problem.

3 RADIATION AND TEMPERATURE EFFECTS IN SPACE ELECTRONICS

3.1 Space radiation environment

The radiation in the space environment is composed of a variety of energetic particles with energies of a wide range from keV to hundreds of GeV and beyond [3]. These

particles are either passing through the space environment or are trapped by the magnetic fields of planets. There are three main sources of the radiation in space [15]:

1. Galactic cosmic rays. These are high-energy charged particles including heavy ions extending to energies beyond TeV. Their fluxes are low, and all ions in the periodic table could be present.
2. Particles generated during solar events (solar flares). Solar eruptions produce a particle cocktail consisting mainly of energetic protons, but there are also alpha particles, heavy ions and electrons in it. The energies could reach hundreds of MeV.
3. Particles trapped inside planets' magnetospheres. These particles form radiation belts around the planets (e.g. Earth, Jupiter). This radiation typically consists of a broad spectrum of energetic particles.

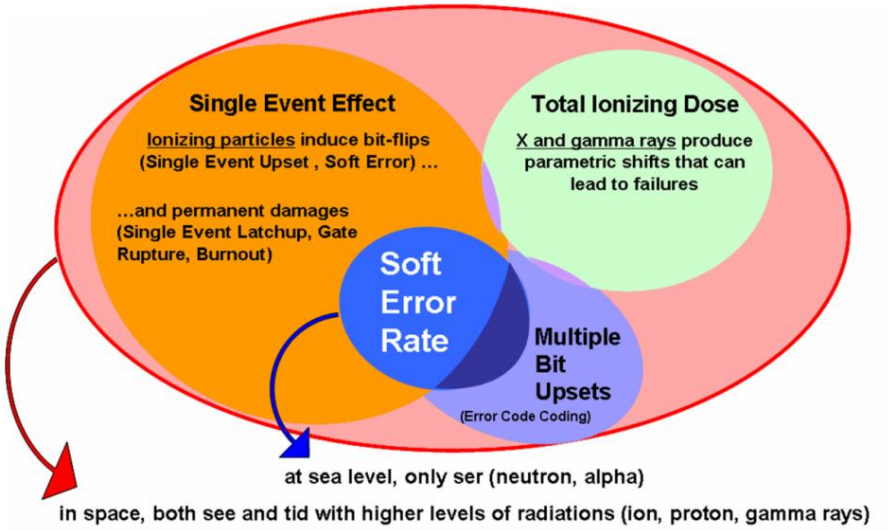

Fig. 3.1: An overview of the family of radiation effects on space electronics and the links between the effects. As the graphics suggest, there is a link between SEEs and TID effects. Figure adapted from [16].

3.2 Radiation effects in space electronics

In general, the space radiation causes two major types of radiation-induced effects in space electronics:

1. Cumulative effects: total ionising dose effects (TID) and displacement damage effects (DD)
2. A wide range of single events effects (SEE).

As can be seen in Fig. 3.1, these effects are partially linked as there have been synergistic effects observed during combined radiation experiments. The TID-induced enhancement of SEE sensitivity is an important synergistic effect for the space electronics industry [17].

3.3 Total ionising dose effects

The TID is cumulative damage induced to the device by exposure to ionising radiation. It typically leads to a degradation ("shift") of device parameters and may end up in its functional failure (in some literature defined as a "catastrophic" failure [18]). The device would typically fail to operate either when its internal compensating circuits are not capable of keeping the device bias points within the designed operational range, or when the increase of the supply current causes a thermal overload of the device. Total dose level is an essential parameter of space rated electronic devices and is defined as TID level, for which the device is still within the specified parameters.

3.4 Total ionising dose effects in bipolar devices

In space electronics, the bipolar junction transistor (BJT) technology is used in both discrete and integrated form. In general, the TID produces degradation of gain and an increase in the leakage currents in BJTs [3].

The traditional vertical structure of an NPN transistor is shown in Fig. 3.2 a). The red dashed line in this figure defines the area where the transistor is the most sensitive to TID: the surface of the base region, where it intersects the overlying oxide [19]. Defects in the silicon/oxide interface over the base have the strongest influence on the sensitivity to the TID. Charge trapped in the base oxide partially inverts the base, which leads to increased collector current, even when the base is biased off [20]. When the base current is increased, the collector current increases less than in a non-exposed device. This effect reduces the current gain.

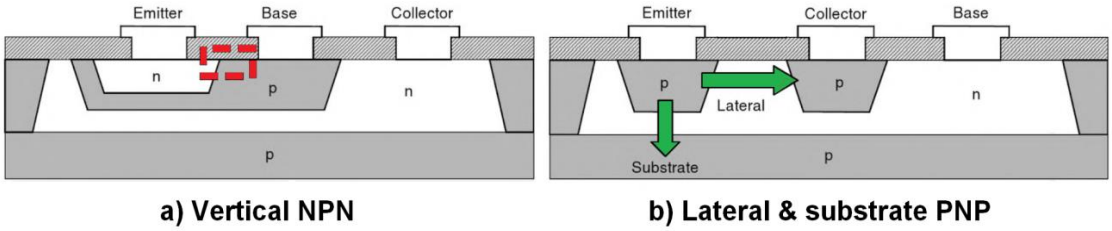

Fig. 3.2: Cross-sections of typical BJT structures: a) shows a conventional vertical NPN transistor; the dashed lines indicate its most radiation-sensitive section. Picture b) represents the lateral and substrate types of PNP. The green arrows indicate the current flow of each type of PNP devices. Illustrations adapted from [21].

3.5 Total ionising dose effects in MOS devices

The metal oxide semiconductor (MOS) technology is the key process of manufacturing modern electronic devices [22], especially in the form of CMOS (Complementary MOS). The key TID-induced problems in a MOS include threshold voltage shift, increased leakage current, and degraded timing parameters [23].

The most crucial TID-induced degradation of MOS devices is the gate threshold voltage shift, as illustrated in Fig. 3.3. During the normal operation (A), the application

of an appropriate gate voltage causes a conducting channel to form between the source and drain so that current flows when the device is turned on. The effect of TID is illustrated in figure (B): TID-induced trapped charge has built up in the gate oxide, causing a shift in the threshold voltage. If this shift is large enough, the device cannot be controlled. This extreme case leads to functional failure of the device [24]. Regarding the construction of commercial devices, the TID-induced charging of the oxide involves several different physical mechanisms.

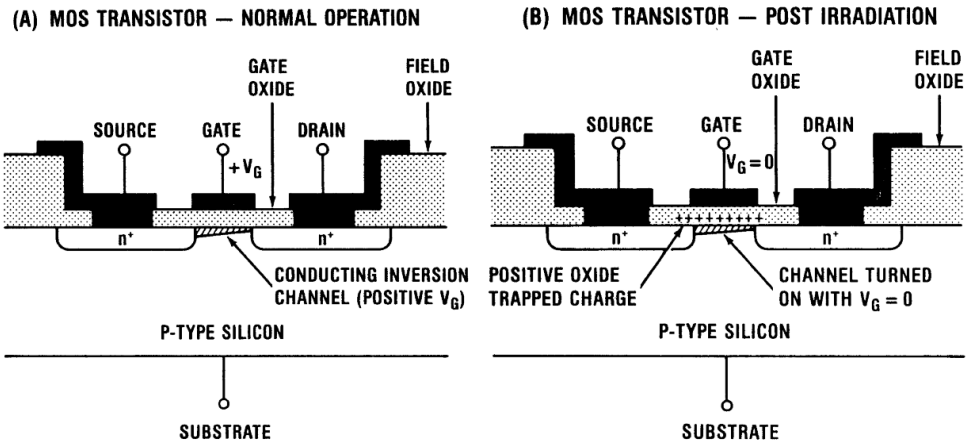

Fig. 3.3: Schematic of the structure of n-channel MOSFET showing the radiation-induced charging of the gate oxide in two modes: (A) normal operation and (B) post-irradiation. Figures adapted from [24].

Two dominant components cause the gate threshold voltage shift [3]:

- oxide trapped charge (also known as charge trapping)
- interface trapped charge (or interface traps)

Typical I_D-V_{GS} curves of irradiated MOSFETs are plotted in Fig. 3.4 to demonstrate the contribution of these two components. While the oxide-trapped charge causes a simple translation of the I_D-V_{GS} characteristics, the interface trapped charge is responsible for both shift and distortion of the curve [3].

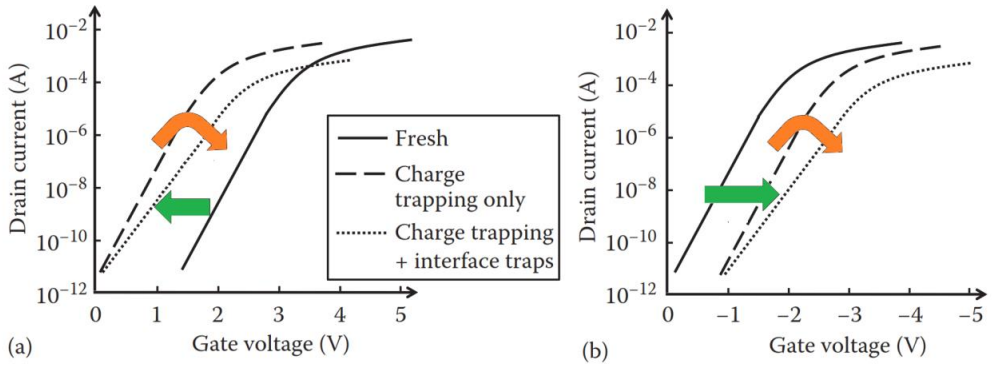

Fig. 3.4: Effect of oxide trapped charge and interface trapped charge on I_D-V_{GS} curves of (a) n-channel MOSFET and (b) of a p-channel type. Charts adapted from [18].

There is a notable difference in the TID response (green arrows in Fig. 3.4) of the n-channel and p-channel MOSFETs. Positive oxide trapping and interface traps cause additive effects in p-channel MOSFETs (orange arrows) because they both tend to shift the I_D-V_{GS} characteristic towards higher V_{GS}. In contrast, these effects tend to cancel in n-channel MOSFET. In CMOS circuits, the different TID response of both the p-channel and n-channel types may cause a degradation of the complementarity of the CMOS.

3.6 Temperature dependence of MOS threshold voltage

The temperature dependence of the threshold voltage TC_{VT} is a complex effect and can be estimated using the following equation [25]:

$$TC_{VT} = \frac{\delta V_T}{\delta T} = \frac{\delta \Phi_{GS}}{\delta T} + 2\frac{\delta \Phi_F}{\delta T} + \frac{\gamma}{\sqrt{2\Phi_F}}\frac{\delta \Phi_F}{\delta T}, \tag{3.1}$$

where ϕ_{GS} is the gate-substrate contact potential, ϕ_F is the Fermi energy and γ is a body effect parameter. Filanovski at al. [25] suggested a TC_{VT} of -0.83 mV/K.

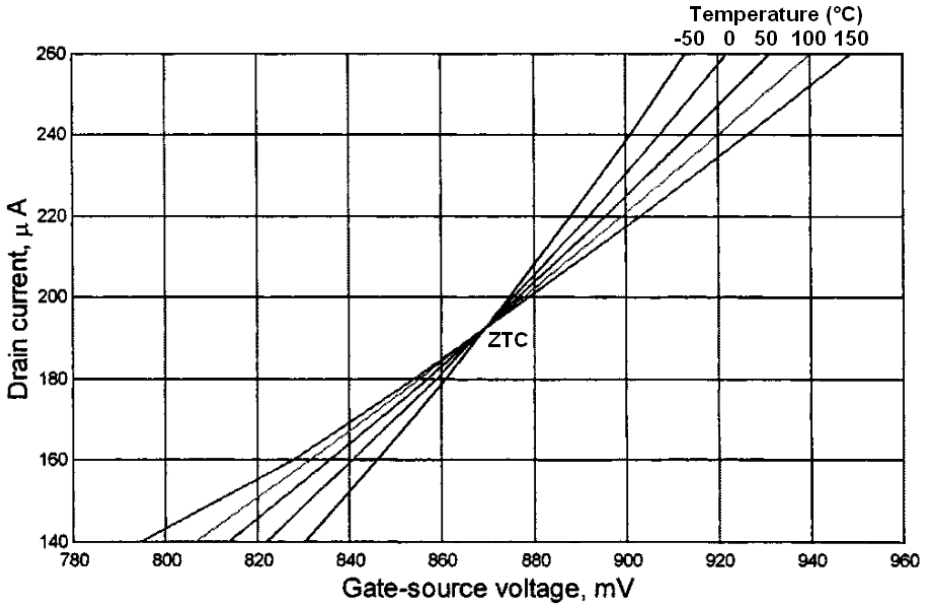

Fig. 3.5: Transconductance characteristics and *ZTC* point of a simulated CMOS n-channel device at various temperatures. The W/L = 50/2.5. Chart adapted from [25].

3.7 Temperature dependence of MOS transistors

The temperature dependence of carrier mobility and threshold voltage are the key contributors to the overall temperature sensitivity of MOS transistors [26], [25]. Their impact on a drain current I_D of an n-channel MOS transistor can be obtained from the

following formula [27]:

$$I_{\mathrm{D}} = \frac{\mu_{\mathrm{n}} C_{\mathrm{ox}}}{2}\left(\frac{\mathrm{W}}{\mathrm{L}}\right)\left(V_{\mathrm{GS}} - V_{\mathrm{T}}\right)^2, \tag{3.2}$$

where μ_{n} is the electron mobility, C_{ox} is the oxide capacitance per area, W is channel width, L is channel length, and V_{GS} is gate voltage. An example of a simulated transconductance of an n-channel 0.35 µm CMOS device is plotted in Fig. 3.5 as a function of temperature [25]. The curves are plotted for temperature steps of 50 °C and are crossing in a point of zero *TC* (*ZTC*), sometimes called *MTC* (minimum *TC*).

3.8 Synergy between TID and temperature

The ambient temperature has a key impact on the TID-induced changes in electronic components [3]. Furthermore, the temperature of the payload aboard a spacecraft can vary significantly [28]. Therefore the synergy between TID and temperature could have a significant impact on the performance of space electronics.

There is a strong connection (synergy) between radiation effects and temperature, including the following effects:

1. irradiation temperature controls the TID-induced changes
2. temperature dependence of the post-irradiation annealing
3. TID-induced change of temperature effects in semiconductors and devices

These effects can be in fact combined; therefore the TID-induced change of temperature effects in semiconductors is also a function of the irradiation temperature. A similar situation is assumed for the annealing of this phenomenon.

4 ADVANCED IN-SITU TID TEST METHODS

The standard bench test is a rather obsolete method for the TID testing. The goal of this section is to give an overview of the in-situ test methods (ISTMs) and discuss the proposed advanced ISTMs that were demonstrated during this PhD research.

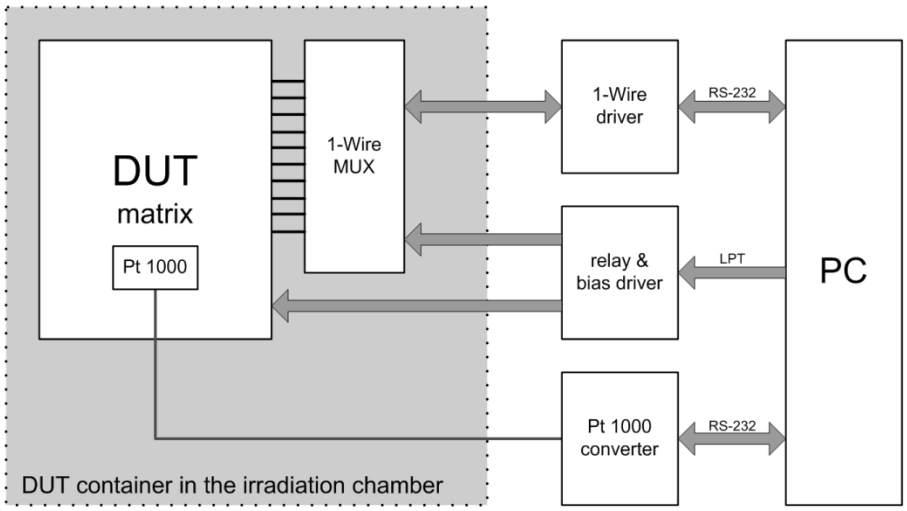

Fig. 4.1: Block diagram of an ISTM ATE. The equipment is divided between the DUT container located in the irradiation chamber and the set of test instruments placed in the laboratory.

4.1 In-situ TID test methodology

The ISTM is frequently based on fully automated test equipment (ATE). This typically consists of a DUT container which is irradiated and a set of test instruments located in a non-radiation area nearby. The two are connected via cables (see Fig. 4.1 for an example of an ISTM ATE). Such a test method brings numerous advantages, including:

- Fully automated testing, i.e. no manual operations are required ("run and forget")
- No limit of measurements duration
- No annealing occurs during measurements
- A higher limit on the number of parameters measured
- A significantly higher amount of data, allowing a detailed data analysis to be made
- The investigation of unknown effects/phenomena
- Temperature monitoring and control
- Precision DUT bias control using switched bias

The major technical challenge of the ISTM ATE is the design of the radiation tolerant electronics which have to be located in the DUT container, due to a limited connectivity between the container and the external set of test instruments. The limiting

factor is the cables. A typical TID irradiation facility requires 15 m length of cables to be placed in the labyrinth inside the concrete shielding. The cables could be a limiting factor for both high speed digital and precision analogue testing.

To conclude, the ISTM ATE system is a rather more complicated concept than the standard test method. However, it is believed that the effort invested in designing and building the ATE is worth it, as the results of such a test are much more objective, and many advanced analyses can be carried out using the resulting data. It is also possible to combine the ISTM method with a standard bench test. Such a hybrid solution can be quite effective, especially for high-speed DUTs for which a pure ISTM test would be either impossible to design or too expensive to build.

4.2 In-situ TID-TC testing

The key technical challenge of the ISTM of the temperature coefficients is to perform the temperature sweep of the DUTs during the irradiation. The standard bench TID tests are typically performed to simulate the full temperature range of the devices using temperature chambers such as Weiss [29]. This method is relatively simple, but has a lot of serious constraints:

- The irradiated devices can be thermally annealed during the *TC* measurement so the radiation-induced changes may be lost due to the long-duration exposure to elevated temperature
- The temperature profile of large chambers might be too slow. Therefore the two hours test window might not be followed [30].
- The repeatability of the *TC* measurements is limited by the accuracy of placing the samples in the chamber and the timing accuracy of the temperature profile.
- Temperature chambers are typically large and expensive (not affordable for low-cost COTS testing)

Modern localised temperature test systems (LTTS) were designed to address the constraints of the traditional testing in temperature chambers. These advanced instruments typically consist of a thermal head, which controls the temperature of the DUTs, and a base unit, that generates the air of stable temperature [31]. During the temperature test, the head is attached to the PCB, and the forced air stream provides the heating or cooling of a single DUT. The LTTS is ideal for bench testing as it allows for fast temperatures changes and good test accuracy/repeatability.

As far as the ISTM testing is concerned, none of the methods described above is suitable. The temperature chambers are too spacious to be placed in the irradiation chamber, and the LTTS contains electronics that would have to be radiation hardened. In both cases, the prices of these instruments are not affordable by low-cost projects.

To address these issues, a novel system for fine DUT temperature control was designed to be used for ISTM testing during this PhD. The system is called DTC (DUT Temperature Controller). As can be seen in Fig. 4.2 the DTC is based on a thermoelectric cooler technology (TEC). The DUTs are attached to a cold side of a multistage TEC using thermally conductive compounds or glues. The cooling of the TEC hot side is provided by a powerful heat sink with attached fans. The temperatures

of the DUTs, as well as the TEC hot side, are monitored using radiation tolerant Pt1000 sensors. The TEC can be operated both in cooling and heating mode by changing the polarity of the DC current [32]. The TEC assembly must be placed in a hermetic container to minimise the humidity of the air around the TEC cold side, and thus suppress frost build-up.

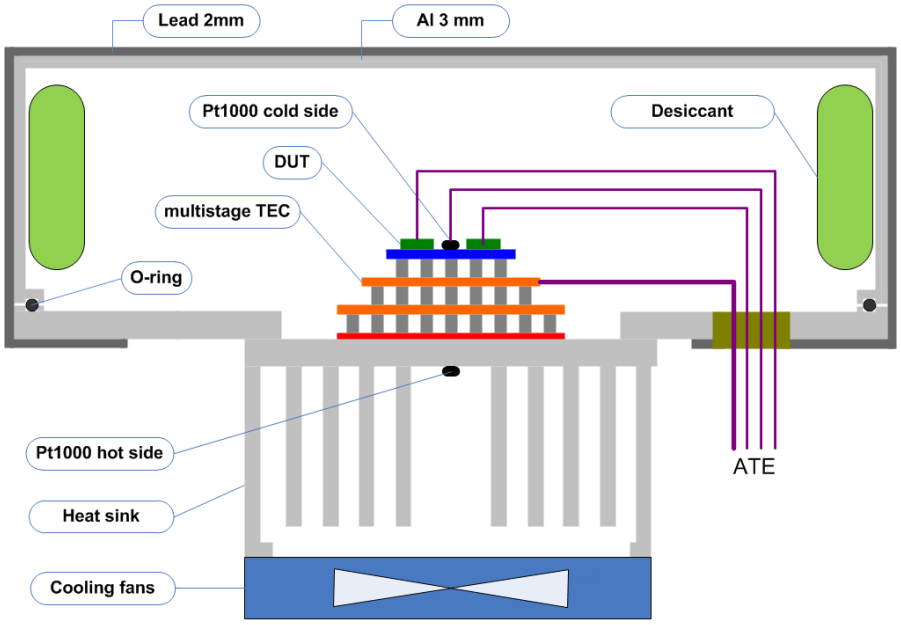

Fig. 4.2: Mechanical structure of the TEC assembly for the ISTM TID-TC testing.

5 PMOS TID-TC EXPERIMENT

5.1 Objectives of PMOS TID-TC experiments

The PMOS TID-TC experiments were performed to meet the following objectives:

1. Measurement of TID-induced threshold voltage shift (responsivity) of commercial PMOS transistors to be used as DUTs and backup TID detectors in the in-orbit experiments
2. Measurement of TID-induced changes of *TC* of PMOS transistors to both demonstrate the ISTM test system (including the DTC system) and obtain TID-TC data for the in-orbit experiments

There were two TID experiments performed during which COTS PMOS transistors were irradiated:

- PMOS1: this was a pilot TID-TC experiment focused on validation of the whole ISTM test system and acquisition of initial PMOS TID-TC data. The PMOS1 experiment was prematurely interrupted due to problems with the test system.
- PMOS2: a full TID-TC experiment using an upgraded test system and an alternative DUT characterisation method.

5.2 The PMOS devices under test

For both PMOS experiments, sets of twenty commercial PMOS transistors of type ZVP1320FPA were used. This type was chosen due to its very low drain current, which made it the lowest power discrete PMOS transistor available on the market. Therefore it was the most similar commercial PMOS transistor to the RADFETS used in previous works [33], [34], [35]. No further DUT production details were available apart from the specification in the datasheet [36]. The DUTs were delivered in the original reel. Therefore it was assumed that the parts were from the same lot. To measure the bias sensitivity of the threshold voltage shift and the *TCs*, the DUTs were divided into five bias groups as defined in Tab. 5.1.

Tab. 5.1: Definition of the bias conditions of the PMOS experiments.

Bias group	DUT numbers	Bias voltage [V]
1	DUT01 to DUT04	0 (GND)
2	DUT05 to DUT08	3
3	DUT09 to DUT12	5
4	DUT13 to DUT16	12
5	DUT17 to DUT20	18

5.3 The test system for the PMOS experiments

The ISTM test system was based on the 2611B SMU (Source Measurement Unit), which performed all measurements. The SMU was combined with a custom-made test controller ISTC1. The ISTC1 provided relay drivers, programmable DUT bias voltage sources and monitoring of the MIF sources. Both the SMU and the ISTC1 were commanded by the test PC. The DUT temperature controller DTC ran independently but was synchronised with the PC every second.

For most of the irradiation time, the DUTs were in the "exposure" mode, i.e. drain (D) and source (S) were grounded, and gate (G) was connected to the relevant bias voltage source via a 100 kΩ resistor. Each bias voltage was generated by an independent circuit consisting of a 16-bit D/A converter followed by an amplifier with low offset voltage and capability of driving high-capacitance loads (cables to the MIF cell). The bias voltages were measured by the SMU and were kept within ±1 mV by programming the D/A converters. These measurements were performed at the beginning of each DUT measurement cycle. The STS software was able to correct bias voltage if it was outside the ±1 mV window. However, this situation was not recorded.

Regular *I-V* curve measurements were made either at the idle temperature of 20 °C or during the temperature sweep, as defined in Fig. 5.1. The DUTs were subsequently switched from "exposure" mode to "reader" mode, during which G and D were grounded, S was driven with a constant current from the SMU, and the S-D voltage (equivalent to DUT V_{GS} voltage) was measured. Sixty current steps were measured from 10 µA to 35 mA. The DUT multiplexing was done via mechanical relays placed in the DUT container near the DUTs. A measurement of one *I-V* curve took 7.5 seconds and, in contrast to [34] and [35], there were no additional delays between setting the drain

current and measuring V_{GS}. The main reason for such a fast measurement was to reduce the time during which the DUTs were exposed to elevated temperatures.

The main sources of measurement error were related to the SMU accuracy. The vendor specified the SMU current source accuracy as 0.03 % of reading + 30 µA and the voltage measurement accuracy as 0.02 % of reading + 5 mV [37]. The SMU was connected using a four-wire circuit, and thus the influence of the cables was minimised.

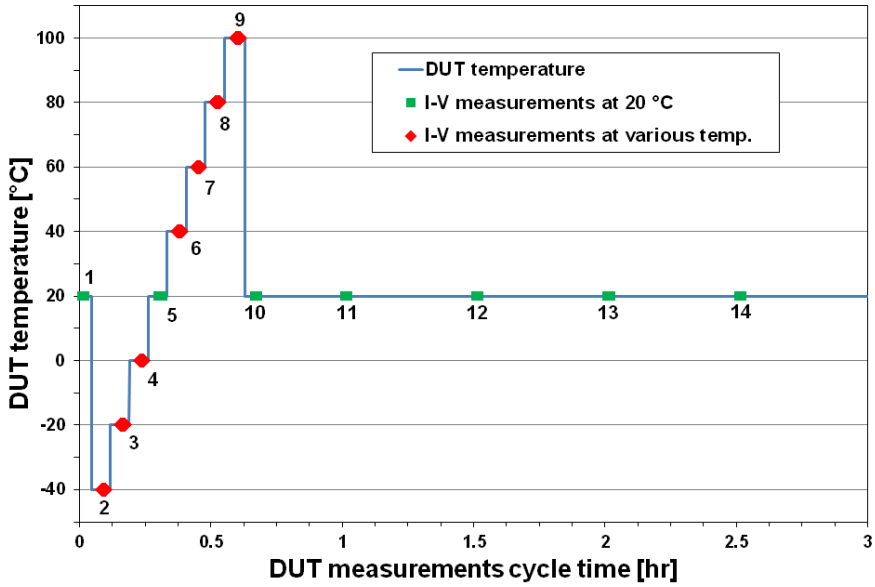

Fig. 5.1: The timing of the DUT measurement cycle, including the temperature profile. DUT *I-V* curves were measured at 20 °C every 30 minutes during the idle time (green squares) and at various temperatures during the temperature sweep (red dots).

The DUTs were attached to the TEC using thermally conductive glue (silver-epoxy compound). To minimise thermal bridges, the DUTs were connected to the multiplexing boards via 100 µm wires.

5.4 The irradiation plan of the PMOS experiments

The MIF (MRC Irradiation Facility) cell 2 was used for the irradiation phase of the PMOS experiments. Cobham RAD Europe operates this cobalt-60 irradiation facility in Harwell, UK.

A dose rate of 360 rad(Si)/hr was used. The dosimetry was performed only prior to the irradiation. There was no dosimetry during the experiment as the mechanical structure of the DUT container did not allow the ion chamber to be placed permanently in the container. PMOS1 experiment idle temperature results

As expected, a TID-induced threshold voltage shift ΔVT was observed for all DUTs. Results for the most sensitive DUTs, using only those data points taken at the idle temperature of 20 °C, are shown in Fig. 5.2.

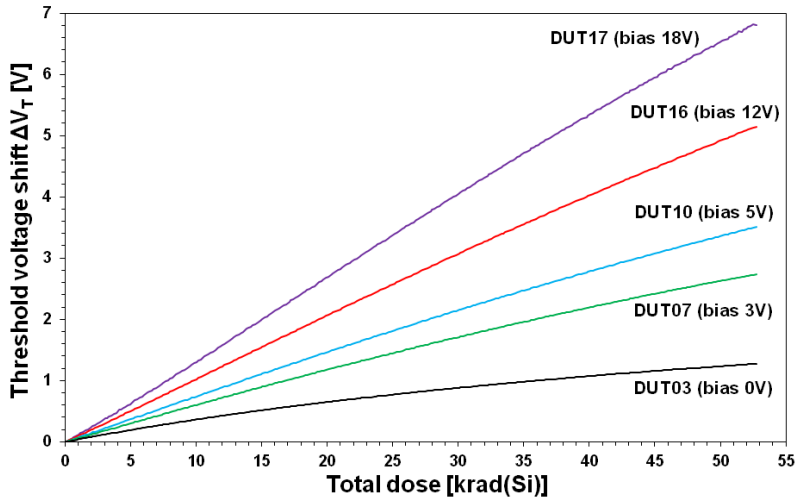

Fig. 5.2: Experiment PMOS1 threshold voltage shift ΔV_T at a drain current of 1 mA plotted as a function of the total dose for selected DUTs at the idle temperature of 20 °C.

The plotted ΔV_T curves were not smooth - a small but consistent ripple can be observed on all DUTs. This effect was one of the problems expected as the DUT temperature was cycled regularly during the irradiation.

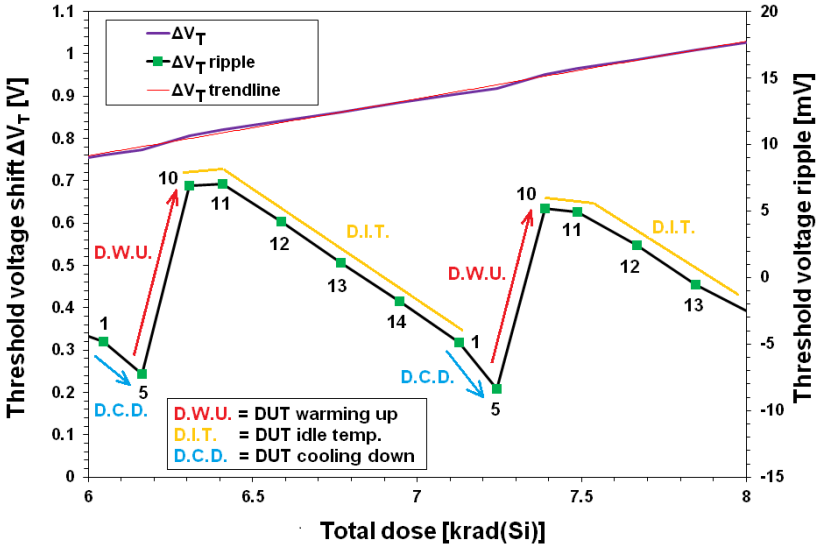

Fig. 5.3: Detail for PMOS1 DUT17 recorded over two DUT measurement cycles, showing that the temperature sweeps significantly alter the ΔV_T values. The ΔV_T curve was fitted with a polynomial function, which was subtracted from the ΔV_T curve to obtain the ripple on it. DUT measurement numbers were added to show the timing.

To analyse this problem, the ripple was "demodulated" from the ΔV_T curves and analysed concerning the timing and DUT temperature profile of the measurement cycle (Fig. 5.3 versus Fig. 5.1). The resulting plot shows that the ripple has an obvious positive temperature dependency. The ripple was not caused by the test method as it was not observed during the pre-irradiation measurements.

The chart in Fig. 5.4 shows the bias voltage dependency of the TID responsivity of the DUTs. A linear regression algorithm was used to calculate the responsivity of each DUT and a coefficient of determination (R^2) was used to compare the linearity of DUT responsivities. A significant difference in R^2 between unbiased and biased devices can be seen.

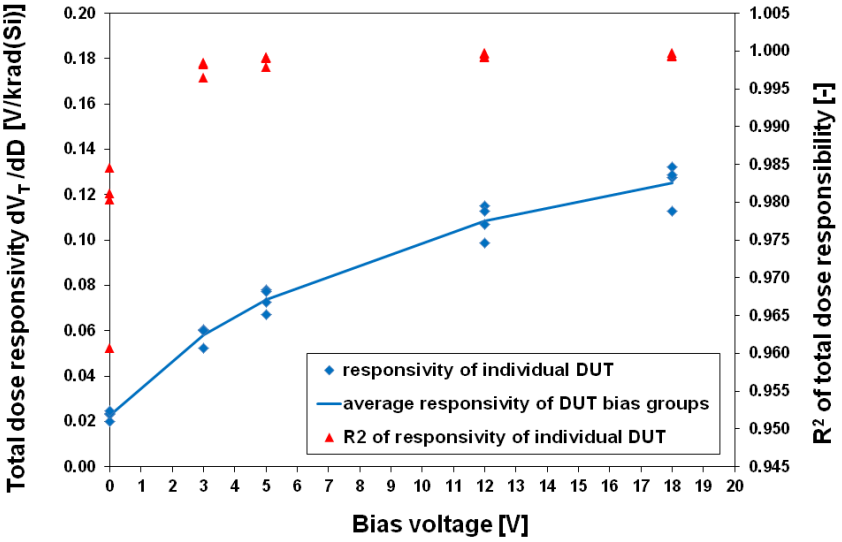

Fig. 5.4: Gate bias voltage dependency of the DUT total dose responsivity as measured during the experiment PMOS1. The individual responsivity of each DUT is plotted as a blue square marker; the blue line represents the average sensitivity of each DUT bias group. The red triangles show the R^2 value for individual DUT responsivities.

5.5 PMOS1 experiment temperature sweep results

As shown in Fig. 5.1, temperature sweep *I-V* curves were measured every three hours (*I-V* 2 to 9), which represents an accumulated dose of 1.08 krad(Si) per measurement cycle. In total, seven temperature steps were used to measure:

- The temperature coefficient of the DUT threshold voltage TC_{VT} [mV/°C]
- The *MTC* point, which represents the value of the drain current at which the magnitude of the TC_{VT} is minimised [mA].

Statistical analysis of the data from the DTC system showed that excellent stability of the DUT temperature control was achieved during the steady moments of the measurements. The accuracy of the *TC* measurements was also improved by the fast response of the DUT temperature controller, allowing compensation of the DUT self-heating. During the *I-V* curve measurements, the stability of the TEC temperature was measured to be within a window of ±0.05 °C. Fig. 5.5 shows a typical record of a DUT temperature sweep measurement.

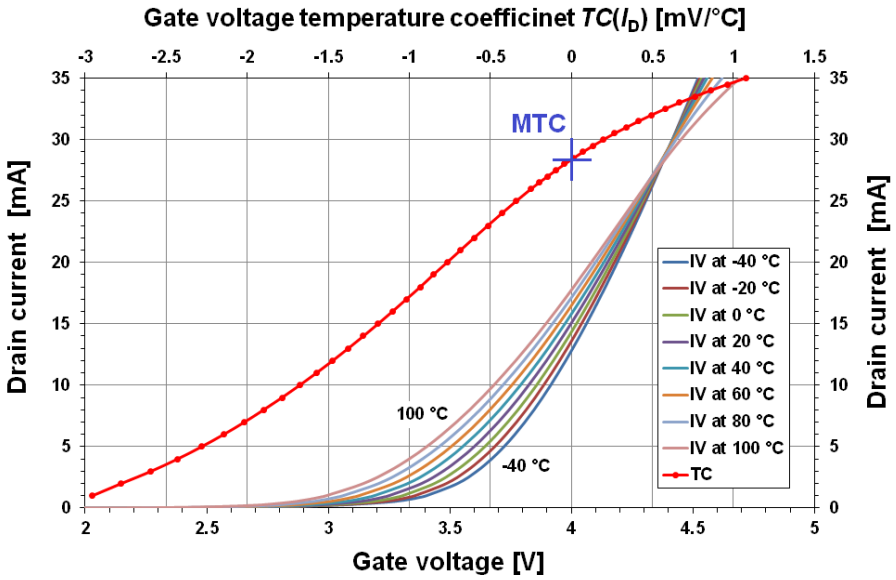

Fig. 5.5: Temperature sweep *I-V* measurements for DUT01 prior to the irradiation of experiment PMOS1. The gate voltage *TC* is plotted as a function of I_D (red line); the red markers show the size of I_D steps. The *MTC* point was at the zero value of the *TC* curve, which was equivalent to I_D at which the *I-V* curves were crossing other.

TID-induced changes in the TC_{VT} were determined at a drain current of 1 mA using 53 measured *I-V* curve data sets. The resulting traces of selected (most sensitive) DUTs shown in Fig. 5.6 exhibit a significant gate bias voltage dependency as well as an initially reversed polarity of the TC_{VT}. The TID-induced changes of the *MTC* points were obtained from the same data using interpolation of two lowest points of the $TC(I_D)$ curves. *MTC* measurements exhibited similar effects to TC_{VT} (Fig. 5.7).

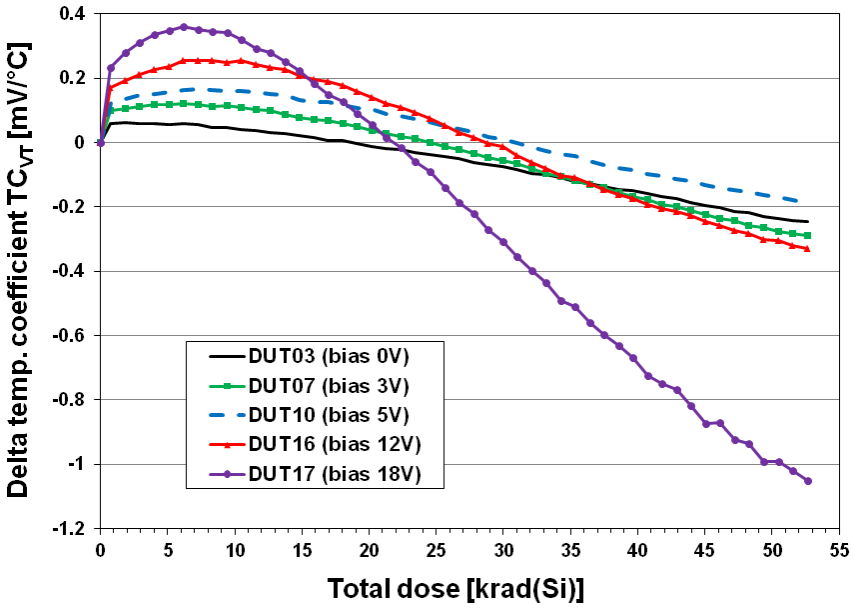

Fig. 5.6: TID-induced changes of TC_{VT} at 1 mA drain current during experiment PMOS1. The markers on the DUT17 curve show the TID resolution of the measurements.

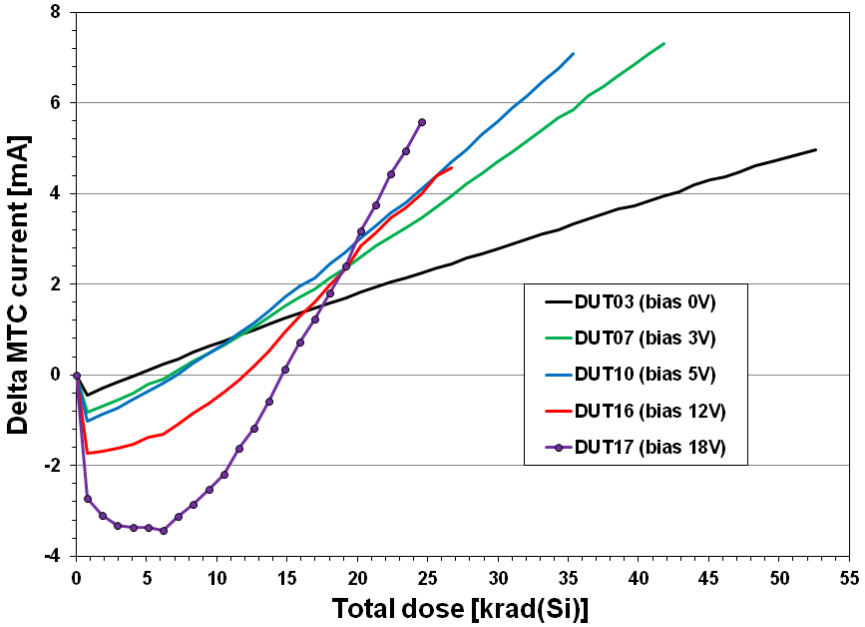

Fig. 5.7: Experiment PMOS1 TID-induced changes of selected DUTs *MTC* points. The markers on the DUT17 curve show the total dose resolution of the measurements. The results were limited by the DUT drain current range of 35 mA.

5.6 Upgrades to the tests system for the PMOS2 experiment

During experiment PMOS1, a fault developed after a total dose of 53 krad(Si) rendering the *I-V* data at higher doses invalid (the voltage readings at I_D > ~10 mA were unstable). To investigate this problem, the DUT container was taken out of the irradiation facility, and the DUTs were bench characterised using the Agilent B1500A semiconductor analyser working in the gate-voltage sweep mode. *I-V* curves measured by the B1500A were normal. The B1500A was later connected instead of the SMU and programmed to mimic the *I-V* curve measurement used in the PMOS1 experiment, and the results were also faulty. It is believed that the cause of this problem was the limited ability of the SMU to drive high capacitive loads (the 15 m cables and the hardware in the irradiation container). A decision was made to upgrade the measurement system for a classical, gate voltage sweep *I-V* curve measurement system and repeat the experiment using a second set of new DUTs that were delivered on the same reel as those used for the PMOS1.

The original test system was extended by adding another SMU (Keithley 2420) to provide a programmable gate voltage source. The SMUs were linked together using synchronisation signals, and a sophisticated embedded test script was developed to allow fast, high resolution, *I-V* curve measurements. Due to this fast embedded control method, the duration of a single *I-V* curve measurement remained the same at 7.5 s. The step size of the gate voltage sweep was 50 mV, and the drain voltage was 15 V during the *I-V* curve measurements. The second measurement method was validated using the irradiated DUTs from PMOS1 and the *I-V* curve data obtained using the B1500A.

The constant drain current method used in experiment PMOS1 allowed the exact programming of the *I-V* curve drain current range. The second method, using the gate voltage sweep, had to be programmed to follow the TID-induced changes in the *I-V* curves continuously. A tracking algorithm was developed to cover this issue: the gate voltage sweep range was calculated prior each *I-V* curve measurement using a trend of a fixed *I-V* curve current point of 30 mA obtained during three previous measurements. The resulting gate voltage sweep range was then extended by 10 % to include a safety margin. This margin helped the algorithm to start smoothly and also compensated for the moderate flattening of the *I-V* curve caused by the TID-induced lowering of the *I-V* curve slope (see Fig. 3.4). This feature was implemented to the STS; the embedded *I-V* curve test script was updated, prior to each *I-V* curve measurement, individually for each DUT. In the case of any problem, a manual adjustment of the algorithm was possible during the experiment. The STS continuously checked the measured *I-V* curves to warn in case of any failure of the algorithm. The timing of the measurements, as well as the temperature profile, remained the same, so the results from experiment PMOS2 could be directly compared to those from experiment PMOS1. The main sources of measurement error were related to the SMU accuracy as for during the experiment PMOS1. The vendor specifies the SMU 2611B current measurement accuracy as 0.02 % of reading + 20 µA and the SMU 2420 voltage source accuracy as 0.03 % of reading + 3.2 mV.

5.7 PMOS2 experiment idle temperature results

Data for total dose up to 150 krad(Si) were analysed from experiment PMOS2. The data were analysed the same way as the results from experiment PMOS1. The data analysis software had to be updated; it employed a high-degree polynomial curve fitting algorithm to obtain the gate voltage values equivalent to the same drain current steps as during experiment PMOS1.

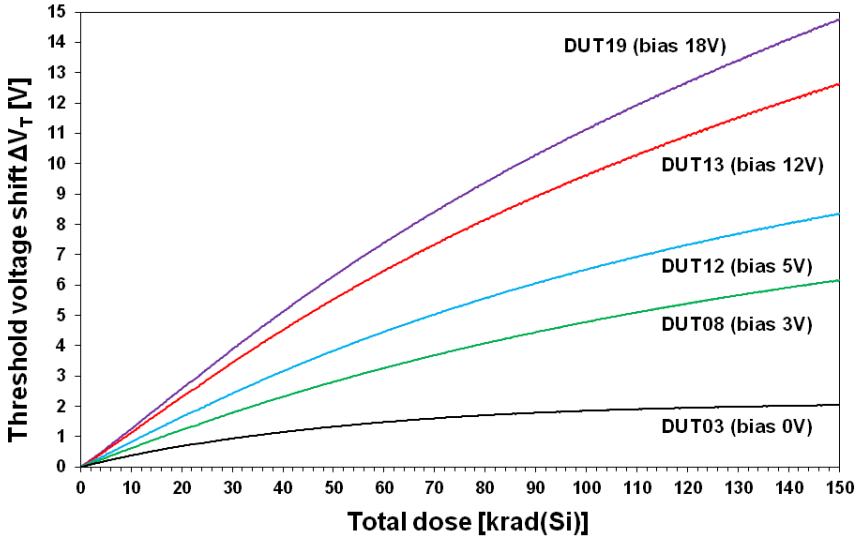

Fig. 5.8: Experiment PMOS2 threshold voltage shift ΔV_T at a drain current 1 mA plotted as a function of the total dose for selected DUTs. All measurements plotted here were taken at the idle temperature of 20 °C.

The TID-induced threshold voltage shift ΔV_T was again observed for all DUTs. A record of the most sensitive DUTs in experiment PMOS2, taken at the idle temperature, can be seen in Fig. 5.8. The initial shifts (up to approximately 50 krad (Si)) in the plotted ΔV_T curves were linear; for doses above this the sensitivity was reduced, and the unbiased DUTs were already saturated at 150 krad(Si). The initial DUT response was nearly identical to the response measured during the experiment PMOS1. The observed ripple was very similar to the ripple measured during the experiment PMOS1 (Fig. 5.3).

5.8 PMOS2 experiment temperature sweep results

The temperature coefficient results from experiment PMOS2 were analysed to obtain plots comparable to those from experiment PMOS1. The TID-induced changes of TC_{VT} were very similar for DUTs within each DUT bias group; therefore average values for each bias group were plotted (Fig. 5.9).

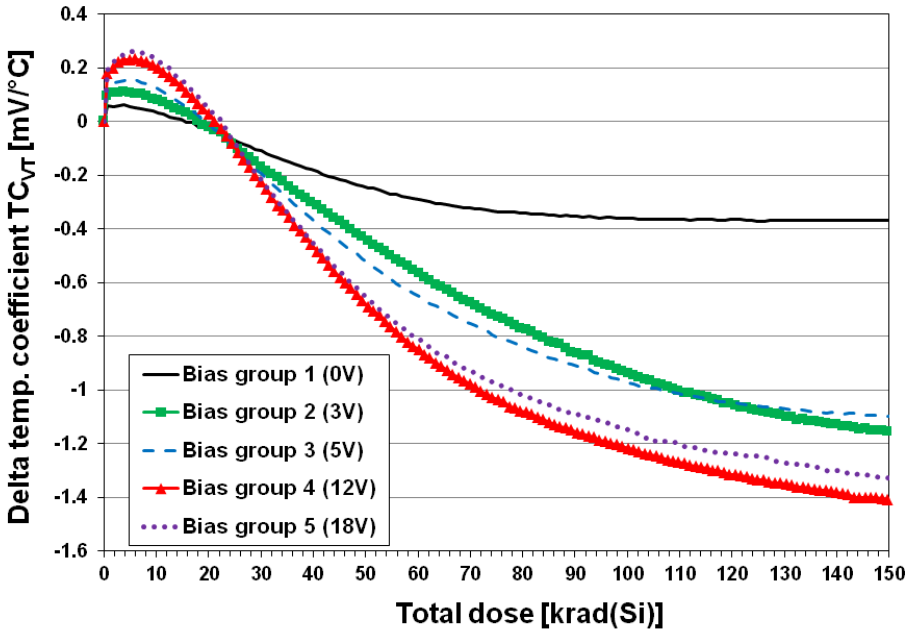

Fig. 5.9: Experiment PMOS2 TID-induced changes of TC_{VT} at 1 mA drain current plotted as an average value for each DUT bias group (four DUTs per group).

The resulting chart shows again that the initial TC_{VT} values were positive and, at a total dose of approximately 23 krad(Si), changed to a negative trend. While the initial positive response had a consistent positive bias dependency, the bias dependency of the negative trend was a more complex function. The initial peak positive TC_{VT} was measured at a total dose of 5 krad(Si), and a bias dependency function was plotted for this particular total dose (Fig. 5.10). The resulting quasi-linear curve was very similar to the bias voltage dependency of the DUT total dose responsivity as measured during the experiment PMOS1 (Fig. 5.4).

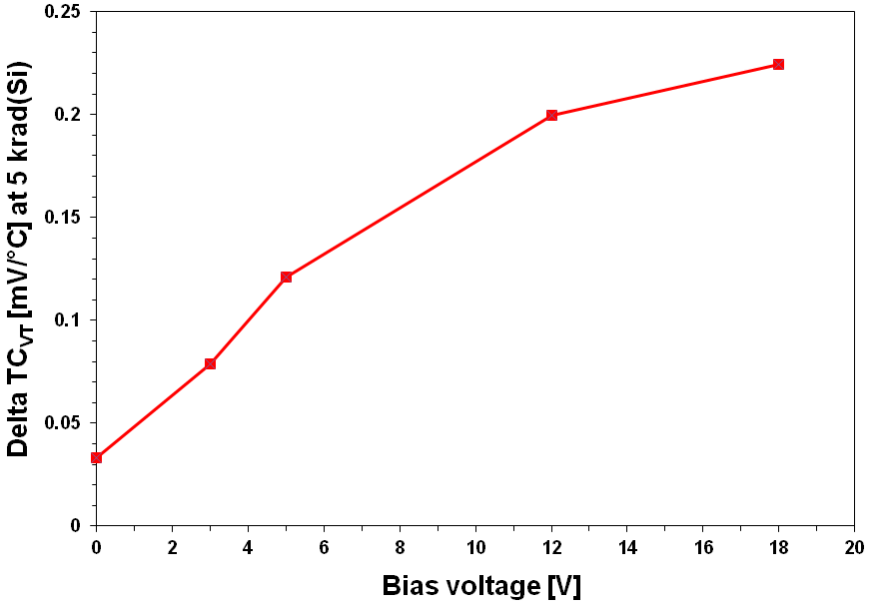

Fig. 5.10: Experiment PMOS2 TID-induced changes of TC_{VT} at 1 mA drain current as a function of bias voltage at the total dose of 5 krad(Si). This chart shows a strong bias sensitivity of the initial (positive) change of the TC_{VT}.

The chart in Fig. 5.11 shows the TID-induced shift in the results of the *MTC* point during experiment PMOS2. The initial negative region was strongly bias dependent, and the peak values were measured at a lower dose of 3 krad(Si).

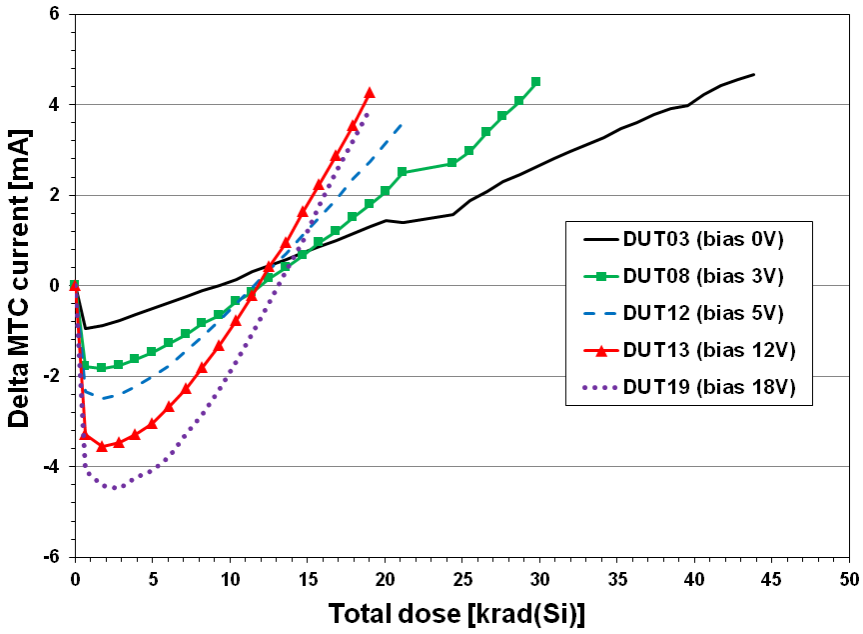

Fig. 5.11: Experiment PMOS2 TID-induced changes of selected DUTs *MTC* points. The results are limited by the drain current range of the DUTs of 35 mA. The pre-irradiation *MTC* points ranged from 29 to 32 mA (initial DUT-to-DUT variation).

5.9 Discussion of PMOS experiments results

The PMOS experiments demonstrated an in-situ test method developed to perform TID experiments and to observe TID-induced changes in temperature effects on a sufficient number of samples. Since there were no radiation test data published for the ZVP transistor series, it was not possible to validate the obtained results. However, the results of this experiment were comparable to data obtained from RADFETs as published in previous papers, including [38]. *I-V* data, collected during the two experiments, showed very good repeatability of this ISTM test system, even if two different *I-V* curve measurement methods were used.

As expected, a strong dependence of all measured parameters on the gate-bias conditions was observed. There was a good agreement of the observed threshold voltage shift bias dependence with irradiation curves published in Fig. 2 of [35]. A significant difference in responsivity was observed between the DUTs (scatter of the blue markers in Fig. 5.4). It is believed that it was not caused by the test method; the variation of the dose-rate across the miniature area of each bias group was negligible, as well as the bias conditions were uniform within each bias group. The DUT-to-DUT variability was probably caused by the limited reproducibility of the manufacturing process [39].

The initially reversed polarity of both the TC_{VT} and MTC curves was not in agreement with the published data for RADFETs (Fig. 20 in [33]). This effect was nearly invisible in the unbiased DUTs. Another interesting result was the positive temperature dependency of the ΔV_T ripple observed on all DUTs. It cannot be explained as concurrent thermal annealing, which was expected to have a negative temperature dependency. Hence the presented data showed temperature accelerated ΔV_T.

The *I-V* curves measured during the temperature sweeps were not symmetrical around the *MTC* point; while the V_{GS} temperature dependency was linear for drain current below *MTC*, it became non-linear above it (Fig. 5.5). This observation was not in agreement with the RADFET result published in [34], Fig. 1. Also, the simulated n-channel MOS device shown in Fig. 3.5 exhibited symmetrical behaviour around the *MTC* point. A possible explanation was a self-heating of the DUT during the *I-V* curve measurement. The RADFETs tested in [34] had a drain current two orders of magnitude lower than the COTS transistors used in this work. This problem was investigated during the B1500A bench tests of the irradiated DUTs from experiment PMOS1. The DUT was still attached to the thermoelectric cooler, and the DUT temperature controller was set for 20 °C. A reversed gate voltage sweep measurement was made, and the resulting *I-V* curve was practically identical to the *I-V* curve from a normal gate voltage sweep. It is believed that this bench test proved that the temperature control is very effective in compensating for the self-heating of the DUT during the *I-V* curve measurement. Therefore, the observed non-linear behaviour above the *MTC* point was most likely a true behaviour of the tested transistor and not an artefact of the measurement method.

The early results of the PMOS experiments were presented at the NSREC 2015 conference, and an extended paper was published in the IEEE-TNS journal [40].

6 CONCLUSIONS

This work was focused on the development of advanced testing methods for evaluation of the impact of the total ionising dose radiation on space data acquisition systems. The long-term goal of this research is to develop ground and in-orbit radiation testing methods that would generate accurate data for various purposes. Firstly, the data can be used for modelling the impact of the TID radiation on the measurement uncertainty of space data acquisition systems. Secondly, the data from combined in-orbit and ground tests can help to improve the understanding of the validity of traditional terrestrial total ionising dose testing. Thirdly, the advanced test methods can make radiation testing affordable to the low-cost NewSpace projects by allowing greater automation of the test process.

6.1 Theoretical background of the work

This thesis contains four chapters dedicated to the theory. Three of them (chapter 2 to 4) were focused on the current theory in the field, and the fourth (chapter 5) summarised the modern trends in space technology and proposals for advanced test methods.

Chapter 2 contains a discussion of the challenges encountered while designing data acquisition systems for space missions and an overview of the process of estimating its measurement uncertainty. A summary of the theoretical background of the space radiation environment, the effects of radiation and temperature on electronic components can be found in chapter 3. The theoretical overview concluded with an outline of traditional radiation hardness assurance and testing (chapter 4).

The final theoretical section (chapter 5) gave an overview of the new era of a commercial approach to space technology (NewSpace) and its impact on the radiation hardness assurance and testing processes. A set of advanced in-situ radiation test methods was proposed to address the requirements of NewSpace and also to provide data with total dose resolution adequate for the development of models that will be used for live estimation of the measurement uncertainties of data acquisition systems during their missions. A concept of such a novel “life mission measurement uncertainty” model concluded the theoretical part of this thesis.

6.2 Development of in-situ test methods and tools

One of the key goals of the presented PhD work was to demonstrate the in-situ radiation testing and evaluate its practical limitations. The in-situ experiments required the development of a variety of special test/measurement methods and tools.

The test systems for experiments were typically based on a combination of high-precision commercial measurement instruments with custom-developed test hardware and software. The aim was to achieve high resolution and accuracy together with reliability. The requirement for the accuracy was driven by the precision of the devices under test and the research of the practical limits of the in-situ test method. Reliability was necessary in order to reduce the risk of an unscheduled interruption of testing,

which would lead to a repetition of the experiment and thus to a loss of valuable radiation testing time and samples.

A series of in-situ test controllers (ISTCs) have been developed to provide a test functionality that was not available within the affordable commercial test solutions. The ISTCs were responsible for: driving the multiplexors; digital communication with the DUTs; monitoring the radiation sources and DUT temperature; generating programmable bias voltages and simulating satellite buses. Five of the ISTC modules have been built, and their robust design led to excellent reliability (no errors were detected during more than three years of operation).

A novel method has been developed for in-situ measurement of radiation-induced changes in temperature coefficients of semiconductors (TID-TC). The need for precise and fast control of the temperature of tested devices led to the development of a DUT temperature controller (DTC). The active part of the DTC (heating/cooling module with the attached samples and temperature sensors) had to be exposed to the radiation during the experiment. To address the special requirements a completely custom solution has been developed and validated during a comprehensive test campaign. The resulting DTC system had excellent parameters (temperature range -40 to 100 °C, with a stability of 0.02 °C, settling time lower than 100 s and measurement uncertainty of 0.4 °C).

The complexity of the PhD experiments led to the development of software for various platforms, including software for the Windows-based PCs, proprietary embedded test controllers (ISTCs, DTCs); COTS test instruments and Linux-based mini-computers. A modular software package called STS (Systematic Test Software) was developed using ANSI C and C++ languages. This meant that the code could be shared between various test platforms.

The developed test system (including the multipurpose STS software package) has also been used for various commercial applications. The majority of them were confidential. However, two of these commercial projects were published. The ISTC and STS technologies were successfully used for heavy ion single event effects testing of RF attenuators [41]. The STS software was also used for characterisation of REM RADFETs for a commercial research program focused on the development of alpha radiation dosimetry [42]. The intended application for this research was monitoring of process stability in the ion implantation process.

6.3 Results of PhD experiments

In general, the TID experiments were performed with the following goals:

- To demonstrate advanced in-situ test methods and evaluate their limits
- To perform novel radiation-temperature testing (TID-TC)
- To improve knowledge of response to TID of various PMOS devices that could be used for in-orbit TID measurements (dosimetry)
- To obtain high-resolution TID-induced degradation data for high-precision commercial data acquisition system components. The TID data would also be used to identify candidate DUTs for in-orbit experiments
- To design and demonstrate an advanced experiment for both terrestrial and in-orbit TID testing of components for precision data acquisition systems.

The very first TID experiment was an in-situ pilot test of digital thermometers DS18B20. It was intended to demonstrate the in-situ technology on relatively simple devices (regarding test instrumentation). The experiment proved that the STS test software and in-situ method could be used for long-term testing, and precision temperature measurements can be performed during irradiation. The experiment also showed the possibility of precise evaluation of the bias sensitivity of the TID-induced degradation.

6.3.1 PMOS devices

In total three various types of PMOS devices were tested during the PMOS experiments (chapter 5): a commercial transistor ZVP1320 was tested together with two types of RADFET sensors (developed by REM and Tyndall). These experiments were designed to improve understanding of the bias dependency of the devices (especially under rather special conditions like a constant current bias), to allow comparison of the responsivity of the devices under identical conditions (both radiation and bias).

The final goal was to measure the TID-induced change of their temperature coefficients using the novel TID-TC method. The obtained TID-TC data showed a significant impact of the radiation on the temperature dependency of the TID readings of the PMOS sensors. The TID-TC results were discussed concerning the current methods of compensation of the temperature sensitivity of the RADFETs – it was demonstrated that the traditional compensation methods should be modified in order to implement the TID-induced change in the temperature coefficients (the current methods assume it is constant).

The PMOS experiments helped to identify the most suitable dosimetry sensors for the planned in-orbit experiment. The best candidates (in terms of the device-to-device variation in responsivity and linearity) were the REM and ZVP1320 devices. However, the Tyndall RADFETs offer significantly lower starting value of threshold voltage and are provided in an SMD package suitable for the limited size of the in-orbit experiment. Therefore the final candidates were the Tyndall RADFETs and ZVP1230s.

6.3.2 Voltage references

A compressive set of experiments has been performed to measure TID-induced changes of various parameters of precision voltage references. Four types of commercial VREF device were chosen to test all modern VREF technologies including bandgap, buried Zener diode and XFET. Low power and small components were used to fit the requirements of the planned in-orbit experiment.

The experiments proved that the TID could significantly change all measured parameters of the VREF devices. These included output voltage (reference voltage) and its temperature coefficient, line regulation, load regulation and supply current. The biased devices appeared to be significantly more immune to TID than the unbiased devices. This was a very important finding for the in-orbit experiment, during which the hardware will be most of the time unbiased. The majority of the devices started to suffer radiation-induced changes from the beginning of the exposure. However, the LT1236 VREF devices (buried Zener diode technology) remained practically unchanged until 10 krad(Si). Such radiation hardness makes these devices interesting candidates

for low-dose missions, such as LEO orbiting satellites. Unfortunately, the LT1236s were not suitable for the planned in-orbit experiment as their supply voltage was too high.

The TID-TC experiment was also performed with the VREF devices. An upgraded test system was developed to address the thermal hysteresis issue with static temperature sweeps - the new test system allowed for the dynamic measurement of the temperature coefficients. The upgrade included a use of an advanced 7.5 digit multimeter, fast multiplexing of the DUTs and dynamic profile of the temperature sweep provided by the DTC controller. The TID-TC results showed that all devices exhibited an initial TID-induced change of the polarity of the TC_{Vo}. In absolute figures, the low doses of radiation were, in fact, lowering the $TC_{Vo,}$ and there was a dose at which the TC_{Vo} was practically zero. A strong bias sensitivity of the VREF devices was confirmed during the TID-TC experiment.

6.3.3 Analogue to digital converters

The final component-level TID experiment in this PhD work was designed to measure TID-induced degradation of two types of high-resolution A/D converters (ADCs). A custom-developed in-situ test system was used to perform all measurements. This solution was also chosen to allow practical demonstration of NewSpace style low-cost testing. The in-situ test system was capable of measuring static parameters (DC errors), DUT supply current and temperature. It could also record waveforms of the digital SPI bus with the DUTs in order to observe potential TID-induced degradation of both static and dynamic parameters of the bus.

Two 24-bit single-channel A/D converters were tested: LTC2400 and AD1251. The noise was the key limiting factor for high-resolution measurements/testing. Therefore the noise performance of the whole signal chain of the ADC tester and the ADCs under the test was measured in-situ in the MIF facility at two stages. These tests concluded that the effective resolution of the designed test system could reach 20 bits, if the raw ADC data is processed using oversampling and averaging, which was very close to the typical effective resolution of the LTC2400 itself.

The TID-induced degradation of the measurement errors of the ADCs were significantly different between the devices; while the LTC2400 started to degrade immediately after the start of the irradiation, the ADS1251 appeared to be immune to the radiation up to a dose of 13 krad(Si) after which it started to degrade practically constantly with the dose.

The ADC TID experiment successfully demonstrated promising capabilities of the designed in-situ test system and reliably measured TID-induced degradation of two COTS 24-bit A/D converters. However, there was not enough data to make final conclusions about the performance of the tested devices as there was only one piece of each type of ADC tested. Despite this limitation, the LTC2400 could be an interesting candidate device for in-orbit testing.

6.3.4 In-orbit experiment

The final chapter in this thesis was focused on the results of the in-orbit experiments developed for in-orbit use during the PhD program. These experiments were called RadEx (short for Radiation Experiments). Two generations of the in-orbit experiments have been developed: the RadEx1 and RadEx2. While the first experiment RadEx1 is described only briefly (due to its cancellation), the second experiment RadEx2 was discussed in detail as it fulfilled objectives of the work planned for the PhD.

The goal of the RadEx2 project was to create a miniature radiation experiment that could be launched on-board an arbitrary satellite including the modern CubeSats. The experiment was designed to perform monitoring of the mission TID level, temperature and precise measurements of degradation of a set of voltage references and the DAQ/test system itself.

Two CubeSat flight opportunities for the RadEx2 have been successfully negotiated, and the schematic of the RadEx2 was integrated with the hardware design of both satellites. An integration package was also created to ease implementation of the RadEx2 with potential future missions.

A comprehensive test plan for the RadEx2 was defined, and it had three stages. The first stage was completed as a part of the presented PhD research, and it was focused on a validation of the design of the experiment and demonstration of its functionality (both regarding the performance of the DAQ hardware and its response to radiation). Prototype hardware of the RadEx2 was built and used as a demonstrator and as a platform for the development of the software library. This software package will be used for ground testing of the experiment and for integration with the satellites.

The second part of the RadEx2 design validation process was an in-situ radiation test, called RadEx2 TID DEMO test. It was performed using hardware and software as similar as possible to the final RadEx2 design and a test controller simulating the satellite bus. The results of the RadEx2 TID DEMO test proved that the RadEx2 experiment could fulfil all planned in-orbit test and measurement tasks. The space segments of the experiments are expected to be launched on-board two CubeSat missions in the 2020's.

6.3.5 Performance of the in-site test method

The results of the various PhD experiments demonstrated that the in-situ test technique can be used even for high-precision measurements of components for advanced high-resolution data acquisition systems.

The reported TID experiments were executed in the MIF facility, which required fifteen-meter cables to interconnect the test instrumentation with the hardware placed inside the irradiation cell. Despite this constraint and a limited budget for the hardware of the test systems, very low noise measurements could be realised.

The initial measurements of the VREF devices showed noise/repeatability better than ±10 μV (±1 ppm at the 10 V measurement range). Also, the data from the ADC tests showed similar results that could be interpreted as 20-bit effective resolution, and RadEx2 had even better results. The repeatability of the measurements of the temperature coefficient was also excellent: it was within ±50 ppb/°C.

6.4 Publications

The presented results of the PhD research were published in various papers and orally presented at workshops and conferences. These results were primarily reported regarding space applications. However, they are also applicable to other fields dealing with the challenges of the radiation effect in electronics. These included high-energy physics, nuclear power research, and medical applications.

The in-situ pilot test of the digital thermometers was presented at the RADECS 2011 conference [43]. The in-situ test method was discussed in a paper which was published at the NSREC 2012 conference [44]. The testing strategy of the early version of the in-orbit experiment (RadEx1) was accepted for a poster presentation at RADECS 2012 [45]. TID testing of the power system for the RadEx1 experiment was presented in an NSREC 2013 paper [46]. The second paper of the 2013 season was dedicated to radiation test of the TEC module for the DUT temperature controller [47]. The TID-TC method was demonstrated on the PMOS transistors. The early results of this experiment were presented at the NSREC 2015 conference, and an extended paper was published in the IEEE-TNS journal [40]. The experimental work continued with testing of the COTS voltage reference devices, which was published at RADECS 2016 conference [48]. A second IEEE-TNS journal paper was published in 2017, and it summarised the results of the TID-TC testing of RADFETs [49]. The final paper, dedicated to the TID-TC experiment with the COTS voltage references, was presented at RADECS 2017 [50]. The early results of the ADC experiment were orally presented at the RADFAC 2017 conference. The 6th Interplanetary CubeSat Workshop (iCubeSat 2017) accepted a talk given on the in-orbit testing experiments [51].

6.5 Future work

The presented PhD research program accomplished its goals. It has been demonstrated, that the TID-induced degradation of commercial DAQ components is a serious problem and that it can be tested with excellent accuracy of measurement and dose resolution by the use of the in-situ technology.

The research program is expected to continue with further development of the test methods and tools, as well as design and execution of advanced experiments. The most important event will be the final ground radiation testing and launch of the RadEx2 experiment. The long-term goal is to obtain two sets of test data: the results of the ground tests and the data from the in-orbit testing. The comparison analysis will show the limitations of the ground TID testing and the true impact of space radiation on the performance of advanced DAQ electronics based on commercial (COTS) components. The data will also be used for the development of the live mission measurement uncertainty (LMMU) models.

The results of this research programme will support the development of future scientific spacecraft. It is also believed, that NewSpace technology has the potential to perform research missions with scientific capabilities comparable to large missions such as the SORCE [52]. The developed of fully-automated test methods can help to provide affordable radiation hardness assurance for these low-cost missions.

REFERENCES

[1] ELVIS, M. What can space resources do for astronomy and planetary science? *Space Policy*. 2016, vol. 37 p. 65–76.

[2] ELVIS, M. The Crisis in Astrophysics and Planetary Science: How Commercial Space and Program Design Principles will let us Escape In *Proceedings of Frontier Research in Astrophysics*. 2016, p. 1–12.

[3] HOLMES-SIEDLE, A., ADAMS, L. *Handbook of radiation effects*, 2/E. Oxford: Oxford University Press, 2002.

[4] FLEETWOOD, D. M., EISEN, H. A. Total-dose radiation hardness assurance. *IEEE Transactions on Nuclear Science*. June 2003, vol. 50, no. 3, p. 552–564.

[5] KEITHLEY *Low Level Measurements Handbook*, 7/E. Cleveland: Tektronix, 2016.

[6] COOMBS, C. F. *Electronic Instrument Handbook*, 3/E. Los Altos: McGraw-Hill, 2000.

[7] ZUMBAHLEN, H. *Linear Circuit Design Handbook*, 1/E. Newton: Analog Devices, 2008.

[8] MA, T. P., DRESSENDORFER, P. V. *Ionizing Radiation Effects in MOS Devices and Circuits*, 1/E. New York: Wiley-Interscience, 1989.

[9] SIERAWSKI, B. D. *et al.* CubeSats and Crowd-Sourced Monitoring for Single Event Effects Hardness Assurance. *IEEE Transactions on Nuclear Science*. January 2017, vol. 64, no. 1, p. 293–300.

[10] KIM, S.-J. *et al.* Model-data comparison of total dose experiment on KITSAT-1. *IEEE Transactions on Nuclear Science*. December 2002, vol. 49, no. 6, p. 2818–2821.

[11] EREN, H. *Electronic Portable Instruments*, 1/E. Boca Raton: CRC Press, 2004.

[12] H. T. CASTRUP *et al. Metrology — Calibration and Measurement Processes Guidelines*, 1/E. Pasadena: NASA Jet Propulsion Laboratory, 1994.

[13] KESTER, W. A. *Data Conversion Handbook*, 3/E. Burlington: Newnes, 2005.

[14] GARRETT, P. H. *Multisensor Instrumentation 6σ Design: Defined Accuracy Computer-Integrated Measurement System*, 1/E. New York: John Wiley & Sons, 2002.

[15] BARTH, J. L., DYER, C. S., STASSINOPOULOS, E. G. Space, atmospheric, and terrestrial radiation environments. *IEEE Transactions on Nuclear Science*. 2003, vol. 50, no. 3, p. 466–482.

[16] BAUMANN, R. Silicon Amnesia: Radiation Induced Soft Errors in Commercial Semiconductor Technology In *Proceedings of the European Conference on Radiation and its Effects on Components and Systems, RADECS*. 2001, p. 23–45.

[17] BUCHNER, S. *et al.* Total Dose Effects on Error Rates in Linear Bipolar Systems. *IEEE Transactions on Nuclear Science*. 2008, vol. 55, no. 4, p. 2055–2062.

[18] BAGATIN, M., GERARDIN, S. *Ionizing Radiation Effects in Electronics - From Memories to Imagers*, 1/E. Padova: CRC Press, 2016.

[19] FLEETWOOD, D. M., SCHRIMPF, R. D. *Defects in Microelectronic Materials and Devices*, 1/E. Boca Raton: CRC Press, 2008.

[20] SCHMIDT, D. M. *et al.* Comparison of Ionizing-Radiation-Induced Gain Degradation in Lateral, Substrate, and Vertical PNP BJTs. *IEEE Transactions on Nuclear Science*. 1995, vol. 42, no. 6, p. 1541–1549.

[21] SCHRIMPF, R. D. Gain Degradation and Enhanced Low-Dose-Rate Sensitivity in Bipolar Junction Transistors. *International Journal of High Speed Electronics and Systems*. 2004, vol. 14, no. 2, p. 503–517.
[22] SPARKES, J. J. *Semiconductor Devices*, 2/E. Milton Keynes: Springer, 1994.
[23] EDMONDS, L. D., BARNES, C. E., SCHEICK, L. Z. *NASA-JPL-00-06 An Introduction to Space Radiation Effects on Microelectronics*, 1/E. Pasadena: NASA JPL, 2000.
[24] OLDHAM, T. R. *Ionizing Radiation Effects in Mos Oxides*, 1/E. Singapore: World Scientific Publishing, 2000.
[25] FILANOVSKY, I. M., ALLAM, A. Mutual compensation of mobility and threshold voltage temperature effects with applications in CMOS circuits. *IEEE Transactions on Circuits and Systems I: Fundamental Theory and Applications*. July 2001, vol. 48, no. 7, p. 876–884.
[26] SZE, S. M., NG, K. K. *Physics of Semiconductor Devices*, 3/E. New Yersey: Wiley & Sons, 2007.
[27] GREGORIAN, R., TEMES, G. C. *Analog MOS integrated circuits for signal processing*, 1/E. New York, 1986.
[28] GILMORE, D. G. *Spacecraft Thermal Control Handbook*, 2/E. El Segundo: The Arospace Press, 2002.
[29] WEISS *Temperature Test Chambers TempEvent Brochure*, 3/E. Balingen: Weiss Umwelttechnik, 2017.
[30] DOD *Test method standard microcircuits MIL-STD-883J TM 1019.9*, 9/E. Washington DC: US Department of Defence, 2013.
[31] MPI *ThermalAir TA-5000 Brochure*, 1/E. New York: MPI Thermal, 2017.
[32] Rowe, D. M. *CRC Handbook of Thermoelectrics*, 1/E. Boca Raton: CRC Press, 1995.
[33] HOLMES-SIEDLE, A., RAVOTTI, F., GLASER, M. The Dosimetric Performance of RADFETs in Radiation Test Beams In *Proceedings of IEEE Radiation Effects Data Workshop*. 2007, p. 42–57.
[34] SARRABAYROUSE, G., SISKOS, S. Behaviour of high sensitivity MOS radiation dosimeters biased in the MTC current region In *Proceedings of the 9th WSEAS Int. Conference on Instrumentation, Measurement, Circuits and Systems*. 2010, p. 38–41.
[35] HARAN, A. *et al.* Temperature effects and long term fading of implanted and un-implanted gate oxide RADFETs In *Proceedings of the 7th European Conference on Radiation and Its Effects on Components and Systems (RADECS)*. 2003, p. 465–469.
[36] ZETEX *ZVP1320F Datasheet*, 4/E. Plano: Diodes Incorporated, 2012.
[37] TEK *Series 2600B System SourceMeter Instrument Reference Manual*, 2/E. Keithley Instruments, 2013.
[38] HOLMES-SIEDLE, A., ADAMS, L. RADFET: A review of the use of metal-oxide-silicon devices as integrating dosimeters. *International Journal of Radiation Applications and Instrumentation. Part C. Radiation Physics and Chemistry*. 1986, vol. 28, no. 2, p. 235–244.
[39] GUILLERMIN, J. *et al.* Part-to-part and lot-to-lot variability study of TID effects in bipolar linear devices In *Proceedings of 16th European Conference on Radiation and Its Effects on Components and Systems (RADECS)*. 2016, p. 1–8.
[40] HOFMAN, J. *et al.* A Method for In-Situ, Total Ionising Dose Measurement of

Temperature Coefficients of Semiconductor Device Parameters. *IEEE Transactions on Nuclear Science*. December 2015, vol. 62, no. 6, p. 2525–2531.

[41] SHARP, R. E. *et al.* Heavy ion testing of two types of digital step attenuator In *2013 14th European Conference on Radiation and Its Effects on Components and Systems (RADECS)*. 2013, p. 1–4.

[42] SHARP, R. E., HOFMAN, J., HOLMES-SIEDLE, A. Using RADFETs for alpha radiation dosimetry In *Proceedings of 12th European Conference on Radiation and Its Effects on Components and Systems (RADECS)*. 2011, p. 747–750.

[43] HOFMAN, J., SHARP, R. A total ionising dose, in-situ test campaign of DS18B20 temperature sensors In *Proceedings of the European Conference on Radiation and its Effects on Components and Systems, RADECS*. 2011, p. 871–876.

[44] HOFMAN, J., SHARP, R. Measurement Methods for Total Ionising Dose Testing: In-Situ versus Standard Practice In *Proceedings of IEEE Radiation Effects Data Workshop*. 2012, p. 1–4.

[45] HOFMAN, J. In-situ system level TID test of RadEx, a CubeSat class radiation experiment module In *Proceeding of 13th European Conference on Radiation and Its Effects on Components and Systems*. 2012, p. 1–4.

[46] HOFMAN, J. In-Situ, Low Dose Rate, TID Test of the Power Supply Block of RadEx, a CubeSat Class Radiation Experiment Module In *Proceedings of 2013 IEEE Radiation Effects Data Workshop (REDW)*. 2013, p. 1–4.

[47] HOFMAN, J. In-situ, low dose rate, total ionising dose test of the cooling performance of a thermoelectric module In *Proceedings of 14th European Conference on Radiation and Its Effects on Components and Systems (RADECS)*. 2013, p. 1–4.

[48] HOFMAN, J., SHARP, R., HAZE, J. In-situ measurement of total ionising dose induced degradation of various commercial voltage references In *Proceedings of 16th European Conference on Radiation and Its Effects on Components and Systems (RADECS)*. 2016, p. 1–4.

[49] HOFMAN, J. *et al.* In-Situ Measurement of Total Ionising Dose Induced Changes in Threshold Voltage and Temperature Coefficients of RADFETs. *IEEE Transactions on Nuclear Science*. 2017, vol. 64, no. 1, p. 582–586.

[50] HOFMAN, J., SHARP, R., HAZE, J. TID in-situ measurement of temperature coefficient of various commercial voltage references In *Proceedings of 17th European Conference on Radiation and Its Effects on Components and Systems (RADECS)*. 2017, p. 1–4.

[51] HOFMAN, J., HAZE, J., SHARP, R. New techniques for radiation testing of CubeSats In *Proceeding of 6th Interplanetary CubeSat Workshop (iCubeSat)*. 2017, p. 1–21.

[52] ROTTMAN, G., WOODS, T., GEORGE, V. *The Solar Radiation and Climate Experiment (SORCE)*, 1/E. Boulder: Springer, 2006.

CURRICULUM VITAE

WORK EXPERIENCE

2013 – 2018 **Aeroflex/Cobham Rad Europe Ltd** Harwell, UK
2011 - 2013 **Steris Plc.** Harwell, Swindon, UK
Radiation effects research engineer

- design and manufacturing of fully automated test systems for the TID/SEE radiation testing of components and systems for space electronics (both hardware and software)
- responsible for implementation of ECSS/MIL standards and calibration processes
- experimental work on advanced combined total ionising dose/temperature tests of space DAQ electronics (PhD research)
- research of advanced space dosimetry and radiation testing systems (in-orbit testing)
- custom control & dosimetry systems for accelerators and radiation sources

2008 – 2011 **Honeywell HTS CZ, Ltd.** Brno, CZ + Yeovil, UK
HW design engineer, Aerospace Engineering Test Services
Aerospace lab representative, HTS Aerospace division

- general aviation projects (Boeing, Airbus) and military (BAE)
- ATE hardware design and production (COTS and custom HW)
- avionics HW development (rapid prototyping and testing)
- aerospace laboratory (600m^2) responsible engineer (calibrations, safety)
- member of space projects task team (company effort in the European space business, focused on radiation effects)

2005 – 2008 **Honeywell HTS CZ, Ltd.** Brno, CZ + Phoenix, USA
Team Leader, Aerospace Engineering Test Services

- head of a small design team (6 engineers)
- six months of work placement (Boeing 787 flight controls, Phoenix, USA)
- Automated Test Equipment design and production (both HW and SW)
- test requirements identification (test, calibration, device programming)
- avionics development support (design for testability)

2001 – 2004 **Panasonic AVC Networks Czech, Ltd.** Pilsen, CZ
Embedded Software Engineer, TV set R&D department
TV microcontroller software development including:

- devices control via an internal bus, Qlink (TV to DVD communication)
- power supply, protection control, AV switching control, the remote controller

1999 – 2001 **SKODA Controls, Ltd.** Pilsen, CZ

Design Engineer, turbine control systems department

- design of turbine control systems HW based on proprietary PLC
- highly reliable turbine protection systems
- PLC software development
- support of the development of the new generation SKODA PLC

1997 – 1999 **SKODA turbines, Ltd.** Pilsen, CZ

Test Engineer, turbines control systems R&D department

- turbine control system testing at power plants and on test stands
- support of valve actuators and hydraulic regulators development
- data acquisition and analysis systems, sensor calibrations
- development and production of special test electronics

1995 – 1997 **Profess, Ltd.** Pilsen, CZ

Technician – sandwich course (on a weekly rotation)

- assembly and programming of turbine speed and vibration monitoring systems
- process and machinery automation (small PLCs)
- industrial sensors (temperature, pressure, position) setup & calibration

EDUCATION

2011 – present **Brno University Of Technology** Brno, CZ

- PhD programme "**Microelectronics**" – extramural studies, in progress
- topic: **Test methods for evaluation of radiation effects in high precision analogue and mixed-signal devices for space applications**
- research completed, thesis in the final review stage
- expected graduation: Q2 2019

2008 – 2010 **Brno University Of Technology** Brno, CZ

- master programme "**Microelectronics**" – extramural studies
- the programme focused on the design of mixed-signal IC, simulations as well as the technology of hybrid ICs and PCBs (production, population and testing)
- development of advanced DAQ systems
- awarded for thesis: "Photovoltaic panel efficiency measurement system"

2005 **London Institute of Technology and English** London, UK

- course „Business English" (one-month duration)

2005 **TTI School of English** London, UK

- course „General English" (two months duration)

1999 – 2004 **University of West Bohemia** Pilsen, CZ

- bachelor of "**Electronics and IT**" – extramural studies
- certified in Metrology and Diagnostic of Electronic Systems (optional university programme for advanced studies)
- awarded for thesis: The SEMM project - mobile meteorological stations (see External Cooperation above)

1993 – 1997 **Secondary school for Power Industry** Pilsen, CZ

- industrial automation systems technician
- sandwich course in Profess company (mentioned above)